When Particles Meet Nanoindentation: A Novel Strategy for Studying Particle Motion and Particle/Surface Interaction

Regina Fuchs[1], Thomas Weinhart[2], Jan Meyer[1], Hao Zhuang[1], Thorsten Staedler[1], Xin Jiang[1], and Stefan Luding[2]

[1] Institute of Materials Engineering, University of Siegen, Paul-Bonatz-Str. 9-11, 57076 Siegen, Germany

[2] Multiscale Mechanics, Department of Mechanical Engineering, University of Twente, P.O. Box 217, 7500 AE Enschede, The Netherlands

ABSTRACT

A plethora of applications in pharmacy, cosmetics, food industry and other areas are directly linked to the research fields of particle technology and contact mechanics. Here, a typical particle ensemble features particle sizes ranging from the nanometer up to the micrometer regime. Up to date, the direct access to particle motion and particle/surface interaction either requires dedicated homebuilt setups or is limited with respect to the weight of the particle and/or the accessible load regime.

In the work presented here, a novel approach is introduced to overcome some of these limitations by using a nanoindentation setup. In addition to that, we demonstrate a relatively simple experimental path capable of probing sliding, rolling and torsional friction. Basically, the concept of the colloid probe technique, which is well established in the AFM community, is transferred to a nanoindenter setup. The potential of such strategy is shown by studying rolling friction of silica microspheres featuring radii of about 2.5μm, 10μm, 25 and 50μm on various substrates such as Si substrates featuring various roughness as well as flat gold films (300nm film thickness). Key aspects of this work include the influence of surface roughness, adhesion, humidity and the elastic/plastic transition on the rolling of particle over Si and gold surfaces.

INTRODUCTION

The influence of adhesion and capillary forces (humidity), surface roughness and deformation during contact of particles on surfaces plays a central role in many physical, chemical and biological phenomena. Nevertheless, the characteristics of individual particle contacts and details of the deformation of contacting surfaces are still not fully understood. Scanning probe microscopy offers a way to determine particle substrate adhesion [1,2] as well as particle motions [3,4]. Until now, however, all studies of particle substrate contact as well as particle motion either require dedicated self-made setups [5,6] or are limited with respect to the weight of the particle and/or the accessible load regime [7]. Nanoindentation might be a promising technique to shed some light on these issues. In the present work, the idea of the colloid probe technique is transferred to a nanoindenter setup which allows for the preparation of larger particle probes, higher maximum normal load and a unique strategy to sample rolling and torsion of individual particles. In our previous studies [8,9], the capability of this approach to sample sliding, rolling, and torsional friction of individual micron-sized spherical particles has already been demonstrated. Therefore, this work will only focus on three detailed aspects in the context of rolling friction: (i) the deformation of Si and gold surfaces during rolling of individual micron-sized borosilicate spheres, (ii) the influence of surface roughness on rolling and (iii) the

influence of humidity during rolling of different rough micron-sized spheres on rough Si surfaces.

MATERIALS AND METHODS

The contacting surface materials of this study were Si(100) wafers (Siegert Wafer GmbH, Aachen) and flat gold substrates prepared by a template stripping method [10]. To vary the surface roughness of a Si substrate, a plasma etching process was carried out, which has been described in detail in one of our previous studies [8,9]. The template stripped gold surfaces were used as prepared. The RMS roughness of the Si surfaces is 0.3±0.1nm, 1.5±0.2nm, and 2.7±0.4nm, respectively, and the 300nm thick gold film feature a RMS roughness of 0.4±0.1nm. In order to study particle surface interaction, micron-sized borosilicate spheres featuring nominal particle radii of 2.5µm (Duke Standard 9005, Thermo Scientific; mean diameter 5.1±0.5µm, RMS roughness 0.3±0.1nm), 10µm (Duke Standard 9020, Thermo Scientific; mean diameter 17.3µm±1.0µm, RMS roughness 0.7±0.1nm), 25µm (Cospheric LLC, BSGMS-2.2, mean diameter 45-53µm, RMS roughness 17±5nm), and 50µm (Cospheric LLC, BSGMS-2.2, mean diameter 90-106µm, RMS roughness 29±2nm) were used as received. The rolling friction tests were carried out in two procedures. In both cases the borosilicate spheres are placed on the surface of interest prior to testing and individual spheres are contacted with a flat end diamond indenter (20µm diameter, Hysitron Inc.), carefully positioning the indenter tip with its axis aligned with respect to the apex of the spherical particle. The measurements were carried out at room temperature (RT) and 35% relative humidity (RH) using a friction loop fashion with a fixed normal load varying between 3 to 3000µN. In the first type of procedure the scratch length and scratch speed were fixed at 2µm and 1µm/s, respectively. Here only spheres featuring a radius of 2.5µm and 10µm were used. Five individual spheres were selected and tested five times at each normal load. In the second type of procedure particle radii of 10µm, 25µm and 50µm were used. Similar to the first rolling procedure a friction loop method was applied. However, the scratch function was changed in two aspects (i) the friction loop length for each load was set to 5µm and (ii) instead of only one loop an individual sphere experienced a consecutive series of friction loops with normal loads increasing from 3 to 3000µN. In the following this series of friction loops is called cycle. Each sphere was probed for three cycles. Data of five individual spheres were collected and analyzed per cycle. Humidity control was achieved by a home-built setup based on the mixing of dry and humid nitrogen. A variation in RH between 5 and 70% with accuracy better than 0.5% can be achieved. The corresponding measurements were started 30 minutes after the chamber reached the desired humidity level.

RESULTS AND DISCUSSION

<u>Deformation of surfaces during rolling</u>

To study the irreversible deformation of surfaces during rolling, a number of experiments based on the first type of experimental procedure were carried out with sphere radius of 2.5µm on flat Si(100) and 10µm on flat Si(100) as well as a gold surface. The results are shown in Figure 1. A significant change in the correlation between lateral force and applied normal load for the rolling of particle featuring a radius of 10µm on flat Si(100) compared to the other two

cases is observed. While lateral force and applied normal load show a linear interrelationship for rolling of the 10μm spheres on the flat Si(100), both other cases feature a non-linear, second order polynomial, relationship. Such a behavior can be attributed to irreversible processes during the rolling contact [11]. The plastic deformation is obviously even more pronounced for a surface featuring low yield strength such as gold. In order to explore the deformation of the surface after rolling, the residual imprint in gold was estimated by AFM. Here, in order to increase the chance of relocating the rolling position of the sphere on the gold substrate, the friction loop length was set to 5μm. A representative image of such an imprint after rolling is shown in Figure 1. In particular, average values of 4.7±0.4μm and 10±0.6nm were obtained for rolling length and imprint depth, respectively, at a normal load of 600μN. With higher normal load the length stayed constant while the depth increases up to 20nm (at 3000μN normal load). The rolling length agrees well with the friction loop length of the measurement setup. Further studies concerning the details of the plastic deformation of both contact partners are challenging and subject to work in progress.
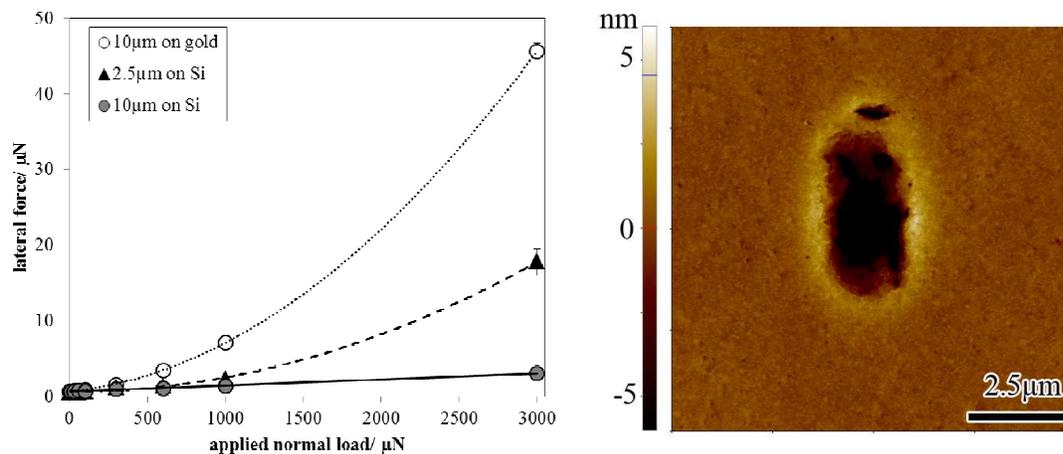

Figure 1. Plot and AFM image of irreversible plastic deformation during rolling contact induced by 2.5μm particle on Si and by 10μm on gold. On the left the resulting lateral force values for rolling measurements are shown and on the right an AFM image after rolling a 10μm sphere on gold with a normal load of 600μN is shown.

The observation of a non-linear relationship between lateral force and applied normal load holds true in case of a predominantly plastic contact. In the next chapter, however, the onset of plastic deformation of asperities within the contact zone will be studied and discussed in detail.

Influence of surface roughness on rolling

We were able to show [8], that rolling friction is presumably adhesion dominated in case of the 10μm spheres in contact with various Si surfaces. In order to take a deeper look at the influence of surface roughness on rolling friction measurement procedure two was employed for spheres featuring radii of 10, 25, and 50μm in contact with the various Si surfaces, respectively. Rolling tests of 10μm spheres on the three different Si surfaces show no significant difference between the individual cycles. Only for the roughest Si surface a slight decrease of about 5% in

the measured lateral force has been observed between the first and third cycle, which presumably indicates an onset of plastic deformation in the asperities of the Si surfaces.

The spherical particles of 25µm and 50µm radii feature significantly increased surfaces roughness compared to the 10µm radii ones. Testing these facilitated access to the influence of surface roughness on rolling friction. Rolling of spheres featuring a 25µm or a 50µm radius, respectively, on flat Si(100) substrates show a non-linear relationship between lateral force and normal load in a low load regime up to 300µN in the first cycle, which we address to a plastic deformation of surface asperities of the sphere. At higher loads the trend changes to a linear one that features the same slope as in case of the second and third cycle. A simple linear trend between lateral force and applied normal load is observed for the second as well as the third cycle. We conclude that the drop in lateral force observed for the second and the third cycle is correlated to the fact that all plastic events associated with surface asperities already took place during the first cycle. Consequent this assumption implies that the surfaces reach an equilibrium roughness after a certain number of cycles. For an ideal elastic/plastic material one cycle should be sufficient. This final state will critically depend on the details of the evolution of roughness, average asperity slope, and average asperity curvature. A detailed analysis is going on and will be reported elsewhere. Nevertheless, we assume that the equilibrium roughness mentioned above will be directly proportional to the real contact pressure between the contact partners at the scale of the corresponding asperities. Consequently the final roughness will most likely decrease with decreasing particle size. In the following chapter, in order to avoid any artifact originating from a change in surface roughness during rolling, we take the third cycle results to get information about the friction coefficient.
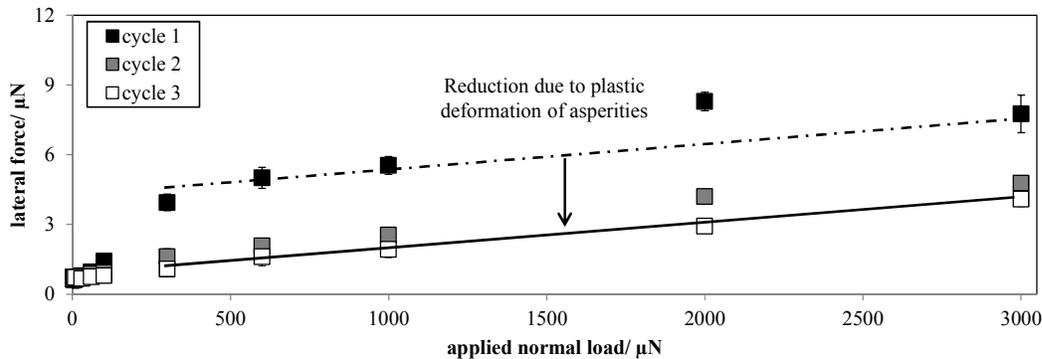

Figure 2. Representative plot obtained from rolling a 25µm sphere on flat Si surface. The first cycle suggest a plastic deformation of surface asperities (for details, refer to the text).

Influence of humidity on rolling

As mentioned above we showed [8] that rolling appears to be adhesion dominated. As adhesive contact forces such as van-der-Waals interactions and water bridges form at the front and break at the backside of the sphere during rolling motion, humidity difference and surface roughness variations should influence rolling friction. In literature, it is well known that capillary forces arise with higher humidity for smooth particle surface contact and moreover, Butt et al. [12] reported the influence of surface roughness and humidity on the adhesion force of small particles on substrates. Small nanoscopic surface asperities on the surface and mesoscopic shape

of the contact zone have a big influence on the adhesion humidity relationship. Inspired by these findings, two particle radii, 10μm and 25μm, and two different Si surfaces (RMS of 0.3±0.1nm and 2.7±0.4nm) are exemplarily used to study the effect of capillary forces and in turn adhesion on the rolling behavior of the particles. Firstly, a smooth 10μm sphere and a rough 25μm sphere are measured on smooth Si to study the influence of humidity and surface asperities of the sphere on the rolling friction coefficient. As mentioned above, even though the 25μm sphere experiences plastic deformation of its surface asperities within the contact zone, it will still feature a larger roughness compared to the 10μm sphere during the third cycle of the test, which is utilized in this study. The results are presented in Figure 3A. A smooth particle in contact with a smooth surface shows a nearly constant value of friction coefficient in the measureable humidity range, which is in good agreement with [12]. The 25μm spheres, however, show a maximum in friction coefficient at around 15% humidity. The surface asperities of such spheres tend to reduce the corresponding meniscus forces between sphere and Si surface. At about RH 15% the water meniscus has reached the height of the asperities and consequently leads to a decrease in the meniscus force with increasing humidity. A decrease in the meniscus force leads, in turn, to a reduced friction coefficient.

Secondly, a smooth 10μm sphere and a rough 25μm sphere were rolled over a Si surface featuring a RMS roughness of 2.7nm. Figure 3B shows a shift of the maximum to higher humidity values. The smooth spheres on the comparable rough Si surface show a maximum at 50%, whereas the rough 25μm spheres on the rough Si surface show a nearly constant value of rolling friction coefficient. Following Butt et al. [12], this finding suggests that in the contact zone of the smooth sphere with the rougher substrate many small nanoscopic asperities exist. For humidity higher than 50% gaps of 2nm width are filled and contribute to the meniscus force. The meniscus force increases until humidity reaches 50% and afterwards it decreases. Again, a decrease in meniscus force is directly associated with a smaller adhesion and, in turn, a smaller friction coefficient. In the case of 25μm spheres we have to consider a combined surface roughness of sphere and surface. Based on the results shown in Figure 3B, it seems likely, that this combination of surface topographies fits in such a way that the contact behaves like two smooth contacting surfaces. Here, a detailed analysis, like mentioned above, depends on information about changes of surface topography of the contacting partners over time, which represents the key target of our current research activities.
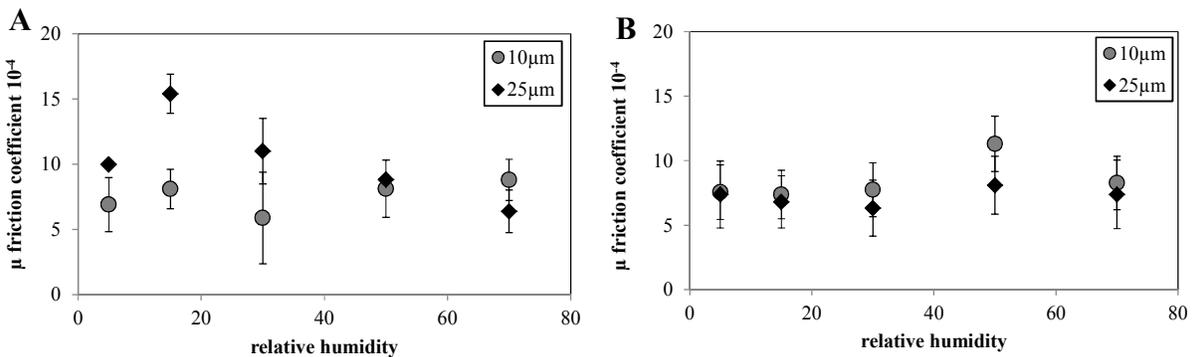

Figure 3. Resulting rolling friction coefficient dependency on relative humidity. A) smooth 10μm and rough 25μm spheres used for rolling on smooth Si. B) smooth 10μm and rough 25μm spheres are used for rolling on Si featuring a surface roughness of 2.7nm.

CONCLUSIONS

We demonstrated the potential of a nanoindenter-based setup to sample and study lateral forces arising during a rolling contact between individual micron-sized spherical particles and various surfaces. It could be shown that it is clearly necessary to distinguish between a predominantly plastic contact and one that only features plasticity on the asperity scale, i.e. within the roughness zone. Furthermore, the setup was sensitive enough to investigate the effect of humidity on the rolling contact of particles and surfaces featuring various radii and roughness in a range between 5 and 70% relative humidity, respectively.
Finally, we were able to identify the determination of the evolution of the topography within the contact zone as factor of paramount importance. Consequently, this finding guides our path in our current research.

ACKNOWLEDGMENTS

REFERENCES

1.   W. A. Ducker, T. J. Senden and R. M. Pashley, Nature **353** (6341), 239-241 (1991).
2.   H. J. Butt, Biophys J **60** (6), 1438-1444 (1991).
3.   M. Sitti and H. Hashimoto, Ieee-Asme T Mech **5** (2), 199-211 (2000).
4.   B. Sumer and M. Sitti, J Adhes Sci Technol **22** (5-6), 481-506 (2008).
5.   W. Ding, A. J. Howard, M. D. M. Peri and C. Cetinkaya, Philos Mag **87** (36), 5685-5696 (2007).
6.   M. D. M. Peri and C. Cetinkaya, J Adhes Sci Technol **22** (5-6), 507-528 (2008).
7.   D. L. Liu, J. Martin and N. A. Burnham, Appl Phys Lett **91** (4) (2007).
8.   R. Fuchs, J. Meyer, T. Staedler and X. Jiang, Tribology - Materials, Surfaces & Interfaces **7** (2), 103-107 (2013).
9.   R. Fuchs, T. Weinhart, J. Meyer, H. Zhuang, T. Staedler, X. Jiang and S. Luding, Granular Matter accepted for publication (2014).
10.   B. Song, W. Walczyk and H. Schonherr, Langmuir **27** (13), 8223-8232 (2011).
11.   J. Tomas, Chem Eng Sci **62** (7), 1997-2010 (2007).
12.   M. Farshchi-Tabrizi, M. Kappl, Y. J. Cheng, J. Gutmann and H. J. Butt, Langmuir **22** (5), 2171-2184 (2006).